Limits on Axions and Axionlike Particles within the Axion Window Using a Spin-Based Amplifier

Yuanhong Wang,[1,2,*] Haowen Su,[1,2,*] Min Jiang,[1,2,†] Ying Huang,[1,2] Yushu Qin,[1,2] Chang Guo,[1,2] Zehao Wang,[1,2] Dongdong Hu,[3] Wei Ji,[4,5] Pavel Fadeev,[4,5] Xinhua Peng,[1,2,‡] and Dmitry Budker[4,5,6]

[1]*CAS Key Laboratory of Microscale Magnetic Resonance and School of Physical Sciences, University of Science and Technology of China, Hefei, Anhui 230026, China*

[2]*CAS Center for Excellence in Quantum Information and Quantum Physics, University of Science and Technology of China, Hefei, Anhui 230026, China*

[3]*State Key Laboratory of Particle Detection and Electronics, University of Science and Technology of China, Hefei, Anhui 230026, China*

[4]*Helmholtz-Institut, GSI Helmholtzzentrum für Schwerionenforschung, Mainz 55128, Germany*

[5]*Johannes Gutenberg University, Mainz 55128, Germany*

[6]*Department of Physics, University of California, Berkeley, California 94720-7300, USA*

(Received 1 February 2022; revised 25 February 2022; accepted 24 June 2022; published 25 July 2022)

Searches for the axion and axionlike particles may hold the key to unlocking some of the deepest puzzles about our Universe, such as dark matter and dark energy. Here, we use the recently demonstrated spin-based amplifier to constrain such hypothetical particles within the well-motivated "axion window" (10 μeV–1 meV) through searching for an exotic dipole-dipole interaction between polarized electron and neutron spins. The key ingredient is the use of hyperpolarized long-lived ^{129}Xe nuclear spins as an amplifier for the pseudomagnetic field generated by the exotic interaction. Using such a spin sensor, we obtain a direct upper bound on the product of coupling constants $g_p^e g_p^n$. The spin-based amplifier technique can be extended to searches for a wide variety of hypothetical particles beyond the standard model.

DOI: 10.1103/PhysRevLett.129.051801

Introduction.—The possible existence of a dark sector of new particles that could mediate exotic long-range interactions between the visible sector of elementary particles is predicted by numerous theories beyond the standard model of particle physics [1–8]. These hypothetical particles weakly coupled to the standard-model particles have been defined as weakly interacting subelectronvolt particles [9], including the most plausible mediators, axions [3,4,10] and the dark photon [11,12]. Axions are introduced as a compelling solution to the "strong CP" problem of quantum chromodynamics [3,4,13,14]. Axions and axionlike particles (collectively referred to as axions) can generically arise in theories at ultrahigh energies, including string theory, grand unified theories, and extra-dimensions models [15,16]. Importantly, axions are prominent dark-matter and dark-energy candidates [17–19] and thus may indeed explain additional puzzling observations, including the rotation curves of galaxies and alignment in the multipoles of the cosmic microwave-background anisotropies [7,12,20,21].

Several theories such as high-temperature lattice QCD [22], the standard model axion seesaw Higgs portal inflation model [23], and axion string networks [24] have predicted that axions, as candidates for cold dark matter, should lie in the mass range of the so-called "axion window" (10 μeV–1 meV) [25–28]. However, existing laboratory searches (e.g., cavity experiments such as the Axion Dark Matter Experiment [29]) and astrophysical observations (e.g., SN1987A [30], white dwarfs [31], and globular clusters [32]) mostly search for axions with masses outside the window. To cover the axion-window gap, a variety of schemes, including the Oscillating Resonant Group Axion experiment [33,34], Magnetized Disk and Mirror Axion experiment [35], Orpheus experiment [36], Axion Resonant InterAction Detection Experiment [37], are proposed and most of their experimental demonstrations are ongoing. Recently, the Oscillating Resonant Group Axion experiment provided new constraints on the axion-photon coupling within the axion window [33,34].

The exchange of axions between fermions results in exotic interactions that may be accessible to laboratory experiments [26,37–57]. Laboratory searches for the axion-mediated interactions could cover the axion window without further hypothesis (the axions are dark matter) or the necessity to scan over this mass range (e.g., the Axion Dark Matter Experiment). Based on the combinations of two vertices for the scattering of two fermions, these interactions were sorted into monopole-monopole (V_{ss}, see [58] for a summary), monopole-dipole (V_{sp}) [26,37–45], and dipole-dipole (V_{pp}) [45–53] interactions. However, due to the difficulty of the extracting sought-after signal from magnetic field, searching for V_{pp} in the axion window remains challenging.

In this Letter, we focus on the exotic dipole-dipole interaction V_{pp} (equivalently V_3 in Dobrescu *et al.* [59]) with $c = \hbar = 1$ [6],

$$V_{pp} = -\frac{g_p^1 g_p^2}{4}\left[(\hat{\boldsymbol{\sigma}}_1 \cdot \hat{\boldsymbol{\sigma}}_2)\left(\frac{m_a}{r^2} + \frac{1}{r^3}\right) - (\hat{\boldsymbol{\sigma}}_1 \cdot \hat{r})(\hat{\boldsymbol{\sigma}}_2 \cdot \hat{r})\left(\frac{m_a^2}{r} + \frac{3m_a}{r^2} + \frac{3}{r^3}\right)\right]\frac{e^{-m_a r}}{4\pi m_1 m_2}, \quad (1)$$

where $g_p^1 g_p^2$ is the product of fermion 1 and fermion 2 pseudoscalar coupling constants for V_{pp}, $\hat{\boldsymbol{\sigma}}_i$ is the spin vector of ith fermion and m_i is its mass, r is the distance between the two interacting fermions, $\hat{r}$ is the corresponding unit vector, m_a is the axion mass. In our actual experiment, a large collection of polarized ^{87}Rb electrons ("spin source") are used as fermion 1 to enhance the exotic signal and polarized ^{129}Xe neutrons ("spin sensor") are used as fermion 2 to detect the signal. Therefore, the product of coupling constants $g_p^1 g_p^2$ studied is $g_p^e g_p^n$. Because the dipole-dipole interaction induces energy shifts of ^{129}Xe spins, the spin sensor can measure the pseudomagnetic field generated by polarized spin-source spins. However, the axion window (10 μeV–1 meV) corresponds to a force range from 0.2 mm to 2 cm in which the spin source generates a significant classical magnetic field on the spin sensor, presenting a challenge of distinguishing the exotic field from it. Former investigations [45,53] focused on the relatively long force range, where the potential V_{pp} falls off exponentially with increasing distance, and thus their constraints were less stringent within the axion window.

In this Letter, we use a spin-based amplifier [10,55] to constrain hypothetical axions within the axion window through searching for the exotic dipole-dipole interaction V_{pp} between polarized electron and neutron spins. This spin sensor employs an ensemble of hyperpolarized long-lived ^{129}Xe nuclear spins as an amplifier for the pseudomagnetic fields from the exotic interactions, which are read out with an atomic magnetometer [60,61]. We demonstrate that the signal from pseudomagnetic fields is enhanced by a factor of more than 40. Using the spin-based amplifier, we obtain a direct upper bound on $|g_p^e g_p^n|$ for pseudoscalars and reach into unexplored parameter space for the axion mass from 0.03 to 1 meV within the axion window. Although demonstrated for the indirect axion searches, our sensing technique can be extended to resonantly search for hypothetical particles beyond the standard model present in the ambient space, such as new spin-1 bosons [55], dark photons [62], and axionlike particles [10].

Spin source.—To search for exotic spin-dependent interaction V_{pp}, we use a spin source (cell 2) consisting of optically pumped ^{87}Rb atoms. The 0.58-cm^3 cell 2 contains a droplet of ^{87}Rb metal and 0.37 amg of N_2 gas. The cell is heated to 180 °C. A 795 nm pump laser [see Fig. 1(a)] tuned to the peak of the D1 transition is amplified with a tapered amplifier and then coupled into a single-mode fiber for optical pumping along $\hat{z}$, delivering approximately 0.5 W of power to the spin-source cell 2. An optical chopper is used to periodically block the pump beam at a frequency $\nu \approx 10.00$ Hz with 50% duty cycle thus modulating the polarization of ^{87}Rb atoms. The modulation frequency is monitored with a photodetector. With pump light on, the polarization of electrons in the whole spin-source cell is averaged over 90% and the corresponding number of polarized ^{87}Rb electron spins is 2.18×10^{14} [63]. The spin-source cell is located 39 mm away from the center of the spin-based amplifier cell (cell 1), as shown in Fig. 1(b).

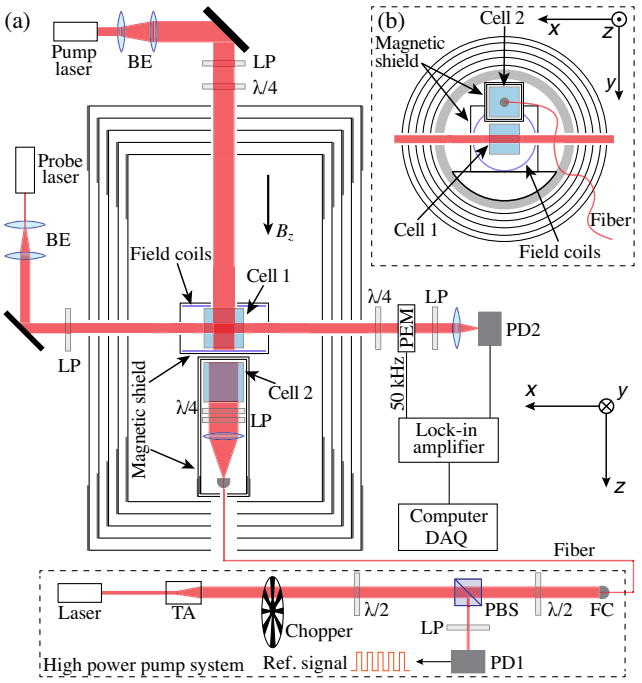

FIG. 1. The experimental setup consists of a spin-based amplifier and a spin source. (a) Experimental schematic in the xz plane. The spin source (cell 2) is shielded by a small-size two-layer magnetic shield. The spin sensor (cell 1) is shielded by a small-size one-layer magnetic shield. Both the source and the sensor are enclosed in five-layer magnetic shield. The cell 1 [60,61,65] containing 5 torr of isotopically enriched ^{129}Xe, 250 torr N_2, and a droplet of ^{87}Rb is heated to 165 °C. The ^{87}Rb spins are polarized with a circularly polarized beam of 795 nm D1 light. ^{129}Xe spins are polarized to ~30% in spin-exchange collisions with polarized ^{87}Rb spins [10,66]. The x component of ^{87}Rb spins is measured via optical rotation of a linearly polarized probe beam, which is detuned to higher frequencies by 110 GHz from the D2 resonance. (b) Experimental schematic in the xy plane. BE, beam expander; LP, linear polarizer; $\lambda/4$, quarter-wave plate; $\lambda/2$, half-wave plate; PD, photodiode; TA, tapered amplifier; PBS, polarizing beam splitter; FC, fiber coupler; PEM, photoelastic modulator; DAQ, data acquisition.

The exotic dipole-dipole interaction V_{pp} between the source electrons and the spin-sensor ^{129}Xe neutrons

mediated by axions generates a pseudomagnetic field on ^{129}Xe spins [55,67],

$$\begin{aligned}\boldsymbol{B}_a &= \frac{g_p^e g_p^n}{16\pi m_1 m_2 \mu_{\mathrm{Xe}}} \int_V \rho(\boldsymbol{r}) \left[\hat{\boldsymbol{\sigma}}_2 \left(\frac{m_a}{r^2} + \frac{1}{r^3}\right)\right. \\ &\quad \left. -\hat{r}(\hat{\boldsymbol{\sigma}}_2 \cdot \hat{r}) \left(\frac{m_a^2}{r} + \frac{3m_a}{r^2} + \frac{3}{r^3}\right)\right] e^{-m_a r} d\boldsymbol{r}, \\ &= \sum_N \boldsymbol{B}_N \cos(2\pi N \nu t + \phi_N), \end{aligned} \tag{2}$$

where μ_{Xe} is the magnetic moment of ^{129}Xe spin, $\boldsymbol{r}$ is the position of the electrons with respect to the sensor, V is the volume of the spin-source cell, $\rho(\boldsymbol{r})$ is the spin density of electrons. Here, we assume the fractional contribution of neutrons in ^{129}Xe spins to be 0.73 [68]. Because of the polarization gradient in the spin source, we use a finite element analysis to evaluate the pseudomagnetic field [63]. Because the ^{87}Rb electron relaxation time (~1 ms) is much shorter than the modulation period (~100 ms), the modulated electron polarization changes quickly and thus the corresponding pseudomagnetic field can be described by a square wave. Based on numerical simulation of Eq. (2), we show that the pseudomagnetic field $\boldsymbol{B}_a$ can be decomposed into several harmonics, i.e., $\nu, 2\nu, 3\nu, \ldots$, where $\boldsymbol{B}_N$ is the Nth field and ϕ_N is its phase [63].

Spin sensor.—To search for these pseudomagnetic fields, we use a spin-based amplifier [10,55,63,69] that employs spatially overlapping ensembles of spin-polarized ^{87}Rb and ^{129}Xe [65], as shown in Fig. 2(a). Hyperpolarized ^{129}Xe nuclear spins act as an amplifier for the resonant signal from pseudomagnetic fields and the ^{87}Rb spins function as a conventional magnetometer to detect the enhanced field. This technique takes advantage of the nuclear magnetic resonance between the modulated pseudomagnetic field $\boldsymbol{B}_a$ and ^{129}Xe spins. When the oscillation frequency of pseudomagnetic fields matches the ^{129}Xe Larmor frequency, the ^{129}Xe spins are slightly tilted away from their polarization axis and generate an oscillating magnetization [10,55,63]. These spins act as a transducer converting the pseudomagnetic field into the effective magnetic field probed with ^{87}Rb spins. Benefiting from the Fermi-contact interactions between ^{129}Xe spins and ^{87}Rb spins, the induced ^{129}Xe transverse magnetization produces an amplified effective magnetic field $|\boldsymbol{B}_{\mathrm{eff}}| \gg |\boldsymbol{B}_a|$ on ^{87}Rb spins [10,55], as shown in Fig. 2. Thus, the spin-based amplifier allows achieving high sensitivity, making it suitable to resonantly search for pseudomagnetic fields generated by V_{pp}. Here, we ignore the pseudomagnetic field along $\hat{z}$ because the spin-based amplifier is insensitive to oscillating fields along this direction.

The amplification effect can be quantitatively described by the amplification factor [10,55,63,69]

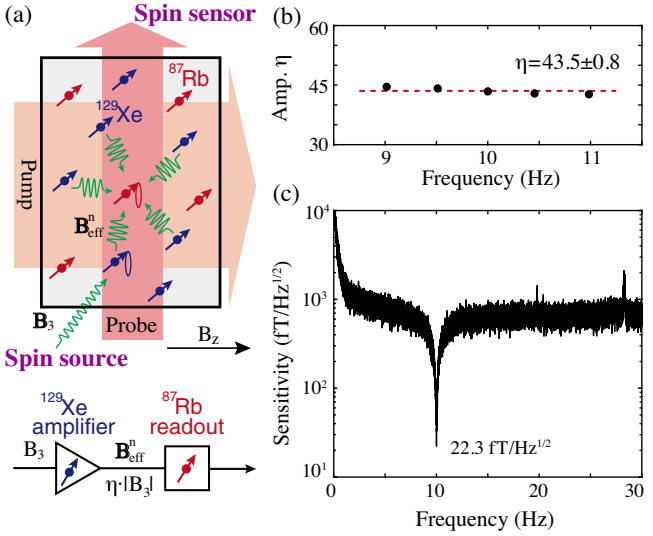

FIG. 2. Magnetic-field amplification of the spin sensor. (a) Principle of using the spin sensor to search for exotic interactions. The signal from the pseudomagnetic field is enhanced by the ^{129}Xe-based amplifier, generating an effective magnetic field $\boldsymbol{B}_{\mathrm{eff}}$ read out by ^{87}Rb spins. (b) The amplification factor 43.5 ± 0.8 is calibrated at frequencies about 9.00, 9.50, 10.00, 10.50, 11.00 Hz. (c) The enhanced magnetic sensitivity reaches 22.3 fT/Hz$^{1/2}$ at resonance frequency 10.00 Hz.

$$\eta = |\boldsymbol{B}_{\mathrm{eff}}|/|\boldsymbol{B}_a| = \frac{4\pi}{3} \kappa_0 M_0^n P_0^n \gamma_n T_{2n}, \tag{3}$$

where κ_0 is the Fermi-contact factor, M_0^n is the maximum magnetization of ^{129}Xe nuclei associated with full spin polarization, P_0^n is the equilibrium polarization of ^{129}Xe nuclei, γ_n is the gyromagnetic radio of the ^{129}Xe nucleus, and T_{2n} is the transverse relaxation time of ^{129}Xe spins. As seen in Eq. (3), considerable amplification requires long transverse relaxation times, high vapor density, and high polarization of nuclear spins. The experiments reported here are performed with a spin-based amplifier similar to that of Refs. [10,55,69], depicted in Fig. 1(a). The ^{129}Xe Larmor frequency is tuned to 10.00 Hz by setting the bias field along $\hat{z}$ at 847 nT. To calibrate the system, an additional oscillating field of 13.0 pT is applied along $\hat{y}$. Scanning the oscillation frequency of this field, we find that the spin-based amplifier responds as a single-pole bandpass filter [10,55] with a full width at half maximum peak amplitude of 49 mHz. Calibration of the amplification factor is performed at several different frequencies between 9.00 and 11.00 Hz with the averaged amplification factor $\eta \approx 43.5 \pm 0.8$, as shown in Fig. 2(b). Therefore, the magnetic sensitivity is enhanced to $\approx$22.3 fT/Hz$^{1/2}$, whereas the off-resonance sensitivity of ^{87}Rb magnetometer is only about 1.0 pT/Hz$^{1/2}$, as shown in Fig. 2(c).

We note that both spin-based amplifiers and self-compensating comagnetometers [48,53,70] use overlapping spin ensembles (e.g., ^{129}Xe – ^{87}Rb), whereas they

are quite different in their frequency response [63]. Comagnetometers operate in a specific bias field, where ^{129}Xe spins and ^{87}Rb spins are strongly coupled [71]. The normal magnetic field is cancelled by the ^{129}Xe magnetization and the ^{87}Rb spins are then in zero-field environment, leaving comagnetometers sensitive to low-frequency exotic fields (e.g., the one modulated at 0.18 Hz in Ref. [48]). In contrast, the spin-based amplifier operates in a broad range of bias fields, where the ^{129}Xe spins and ^{87}Rb are weakly coupled. The effective field generated by the ^{129}Xe magnetization is measured with ^{87}Rb spins, resulting in the sensitivity to pseudomagnetic fields with oscillation frequency above 1 Hz. Therefore, the spin-based amplifier is well suited to searching for new physics predicted by numerous theories beyond the standard model, for example, ultralight axionlike dark matter [10].

Search experiments and data analysis.—Because of the proximity of the spin source to the spin sensor, the source produces a measurable magnetic dipole field on the sensor. The dipole field is calibrated with a commercial miniaturized atomic magnetometer (from QuSpin Inc.) at the position of the spin-sensor cell 1. The magnetic dipole field is measured to be about 3.2 pT with the QuSpin magnetometer, in good agreement with the finite element analysis of magnetic field [63]. To eliminate the magnetic dipole field, the spin source is shielded with two-layer μ-metal shields and the spin sensor is shielded with a one-layer μ-metal shield, as shown in Fig. 1(a). The total shielding factor is experimentally determined to be $> 10^6$, and thus the dipole field is reduced to < 3.2 aT, which is negligible with respect to the magnetic sensitivity in our experiment.

During the experiment, the spin-based amplifier is tuned to resonance frequency to match the optical chopping frequency of the spin-source pump laser, i.e., $\nu_0 \approx \nu \approx 10.00$ Hz. Because of the narrow bandwidth (49 mHz) of the amplifier, only the first harmonic of the pseudomagnetic fields is amplified [see Eq. (2)] and the effect of other harmonics is negligible [63]. The data were collected in six-hour batches, after which the spin-based amplifier was readjusted to optimize the magnetic-field sensitivity by tweaking the bias field, etc. While recording search data, the parameters of the spin source were monitored, such as the chopper frequency and pump power. The total duration of the search experiment was about 24 hours.

In data analysis, a "lock-in" scheme is used to extract the weak signal with a known carrier frequency from noisy environment [54,55]. The reference frequency for this procedure is given by the chopper frequency, and the phase is measured by applying an auxiliary oscillating magnetic field with a coil. The weak signal of the spin-based amplifier is separated into segments of a single period ≈0.1 s and a corresponding experimental coupling strength $|g_p^e g_p^n|/4$ is extracted. A histogram of such coupling strength and a corresponding Gaussian fit is obtained to provide the mean value and standard error for each record (1 hour), as shown in Fig. 3. The final coupling strength is obtained as $|g_p^e g_p^n|/4 \approx (5.3 \pm 48.5_{\text{stat}})$ for $m_a = 0.1$ meV with a weighted reduced chi-square $\chi^2 = 1.65$. The details are presented in Sect. V of the Supplemental Material [63].

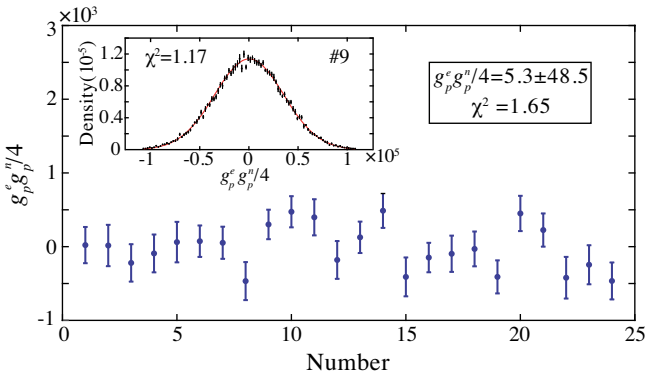

FIG. 3. Experimental coupling strength at $m_a = 0.1$ meV. Each point and its error bar represent the average of one hour and its corresponding standard error over approximately one hour, respectively. The weighted reduced chi-square is $\chi^2 = 1.65$. Inset top: Graph of values for each 3600 s-long record closely follows a Gaussian distribution for 9th hour data with $\chi^2 = 1.17$.

Systematic errors are summarized in Table I. It was found that one of important contributions to the uncertainty comes from the phase variation of the reference signal after reoptimizing the sensitivity of the spin-based amplifier. Another important contribution is from the calibration constant α, the coefficient transferring the output signal (V) of the spin-based amplifier to the unknown pseudomagnetic field (nT). The fluctuation of α can be caused by the intrinsic instability of the spin-based amplifier, including the fluctuation of the laser beam and temperature and the instability of the modulation frequency ν of the chopper. In the future, replacing the optical chopper with acousto-optic or electro-optic modulators can significantly improve

TABLE I. Summary of corrections to $|g_p^e g_p^n|/4$ (presented here for $m_a = 0.1$ meV) and systematic errors.

Parameter	Value	$\Delta g_p^e g_p^n/4$
Position of cell $2x$ (mm)	1.9 ± 0.2	$^{<0.01}_{-0.04}$
Position of cell $2y$ (mm)	-23.1 ± 1.0	$^{-0.98}_{+1.23}$
Position of cell $2z$ (mm)	41.9 ± 0.3	$^{+0.75}_{-0.69}$
Number of polarized Rb (10^{14})	2.18 ± 0.18	$^{-0.41}_{+0.44}$
Phase delay ϕ (deg)	102.6 ± 0.6	$^{-1.45}_{+1.45}$
Calibration constant α(V/nT)	$2.11^{+0.002}_{-0.386}$	$^{-0.01}_{+1.20}$
Final $\lvert g_p^e g_p^n\rvert/4$	5.3	±48.5 (statistical)
($m_a = 0.1$ meV)		±2.4 (systematic)

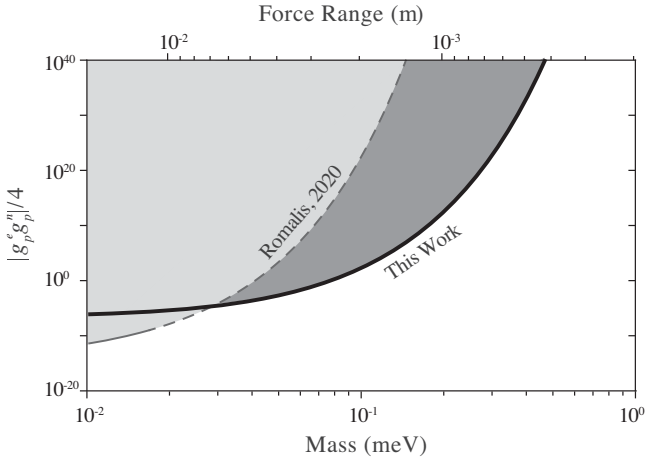

FIG. 4. Experimental constraints on $|g_p^e g_p^n|/4$ within the axion window. The thick dark curve represents the experimental limits on the electron-neutron coupling with 1.96σ uncertainty as a function of the boson mass m_a in the bottom axis and the force range $\lambda = \hbar(m_a c)^{-1}$ in the top axis. The thin gray curve indicates the same coupling derived from comagnetometer experiments [53], while the dashed one is deduced based on Eq. (1). Our limits set new constraints on axions or axionlike particles for $m_a > 0.03$ meV within the axion window.

the stability of the modulation frequency, which could further reduce systematic errors. The number of polarized ^{87}Rb spins and its corresponding standard error $(2.18 \pm 0.18) \times 10^{14}$ is characterized by the parameters of the spin source, such as the optical absorption, the atomic density, and the size of the cell 2. The overall systematic uncertainty is derived by combining all the systematic errors in quadrature [63]. Accordingly, we quote the final total coupling strength $|g_p^e g_p^n|/4$ as $(5.3 \pm 48.5_{\text{stat}} \pm 2.4_{\text{syst}})$ at $m_a = 0.1$ meV.

Figure 4 shows the new constraints on $|g_p^e g_p^n|/4$ set by this work together with recent constraints from experimental searches for exotic dipole-dipole interactions within the axion window [53]. The solid line represents the constraints of our work, corresponding to 1.96 times the quadrature sum of the statistical error and systematic error (95% confidence level). The comagnetometer experiment placed direct constraints on $|g_p^e g_p^n|/4$ in the range of $m_a < 20$ μeV. These limits are further extended in our work to constrain higher mass axions and presented as the derived dashed line [53], which decrease exponentially with the mass m_a within the axion window. For the mass range from 30 μeV to 1 meV, we set the most tight constraints on $|g_p^e g_p^n|/4$. Our limits significantly improve over previous deduced constraints. Importantly, our work bridges the gap between the existing laboratory searches [29] and astrophysical observations [30–32], opening a route toward exploring new parameter spaces in the axion window.

In conclusion, we report new direct constraints, based on a spin-based amplifier, on $|g_p^e g_p^n|/4$ by exploring the axion-mediated dipole-dipole interaction within the well-motivated axion window. A further improvement of the experimental sensitivity to exotic interactions is anticipated. For example, the use of ^{3}He-based amplifier that has much longer spin-coherence time than that of ^{129}Xe [48] could improve search sensitivity by several orders of magnitude [10,55]; further, solid-state spin sources such as optically pumped pentacene crystals [72] could increase the polarized electron number density by more than 4 orders of magnitude. Although demonstrated for electron-neutron coupling $|g_p^e g_p^n|/4$, neutron-neutron pseudoscalar coupling $(g_p^n)^2$ can also be searched by using nuclear-spin sources such as noble gas vapor cells [10] and para-hydrogen-enhanced liquids [73]. Moreover, the spin-based amplifier can be generically applied into resonant searches for other new particles beyond the standard model—for example, spin-1 bosons such as paraphotons and Z' bosons [55,74] or dark photon [62,75]. These bosons can mediate exotic spin-spin velocity-dependent interactions (V_{6+7}, V_8, V_{14}, V_{15}, and V_{16}). Combining our current ^{129}Xe-based amplifier and recently developed $SmCo_5$ spin sources [53,54], we may provide the highest sensitivity in the search for light bosons in the mass range from 0.01 to 1 meV.

We thank Mikhail Kozlov and Yuzhe Zhang for valuable discussions. This work was supported by National Key Research and Development Program of China (Grant No. 2018YFA0306600), National Natural Science Foundation of China (Grants No. 11661161018, No. 11927811, No. 12004371), Anhui Initiative in Quantum Information Technologies (Grant No. AHY050000), USTC Research Funds of the Double First-Class Initiative (Grant No. YD3540002002). This work was also supported by the Cluster of Excellence "Precision Physics, Fundamental Interactions, and Structure of Matter" (PRISMA + EXC 2118/1) funded by the German Research Foundation (DFG) within the German Excellence Strategy (Project ID 39083149).

*Y. W. and H. S. contributed equally to this work.
†Corresponding author.
dxjm@ustc.edu.cn
‡Corresponding author.
xhpeng@ustc.edu.cn

[1] D. DeMille, J. M. Doyle, and A. O. Sushkov, Probing the frontiers of particle physics with tabletop-scale experiments, Science **357**, 990 (2017).
[2] N. F. Ramsey, The tensor force between two protons at long range, Physica (Amsterdam) **96**, 285 (1979).
[3] F. Wilczek, Problem of Strong P and T Invariance in the Presence of Instantons, Phys. Rev. Lett. **40**, 279 (1978).
[4] R. D. Peccei and H. R. Quinn, *CP* Conservation in the Presence of Pseudoparticles, Phys. Rev. Lett. **38**, 1440 (1977).

[5] S. Weinberg, A New Light Boson?, Phys. Rev. Lett. **40**, 223 (1978).

[6] P. Fadeev, V. Y. Stadnik, F. Ficek, M. G. Kozlov, V. V. Flambaum, and D. Budker, Revisiting spin-dependent forces mediated by new bosons: Potentials in the coordinate-space representation for macroscopic-and atomic-scale experiments, Phys. Rev. A **99**, 022113 (2019).

[7] M. S. Safronova, D. Budker, D. DeMille, Derek F. Jackson Kimball, A. Derevianko, and C. W. Clark, Search for new physics with atoms and molecules, Rev. Mod. Phys. **90**, 025008 (2018).

[8] J. Moody and F. Wilczek, New macroscopic forces?, Phys. Rev. D **30**, 130 (1984).

[9] H. Yan and W. Snow, New Limit on Possible Long-Range Parity-Odd Interactions of the Neutron from Neutron-Spin Rotation in Liquid ^{4}He, Phys. Rev. Lett. **110**, 082003 (2013).

[10] M. Jiang, H. Su, A. Garcon, X. Peng, and D. Budker, Search for axion-like dark matter with spin-based amplifiers, Nat. Phys. **17**, 1402 (2021).

[11] J. Jaeckel and A. Ringwald, The low-energy frontier of particle physics, Annu. Rev. Nucl. Part. Sci. **60**, 405 (2010).

[12] P. Langacker, The physics of heavy Z' gauge bosons, Rev. Mod. Phys. **81**, 1199 (2009).

[13] J. E. Kim and G. Carosi, Axions and the strong CP problem, Rev. Mod. Phys. **82**, 557 (2010).

[14] Z. Berezhiani and M. Y. Khlopov, Cosmology of spontaneously broken gauge family symmetry with axion solution of strong CP-problem, Z. Phys. C **49**, 73 (1991).

[15] I. G. Irastorza and J. Redondo, New experimental approaches in the search for axion-like particles, Prog. Part. Nucl. Phys. **102**, 89 (2018).

[16] P. Svrcek and E. Witten, Axions in string theory, J. High Energy Phys. 06 (2006) 051.

[17] J. Preskill, M. B. Wise, and F. Wilczek, Cosmology of the invisible axion, Phys. Lett. **120B**, 127 (1983).

[18] L. F. Abbott and P. Sikivie, A cosmological bound on the invisible axion, Phys. Lett. **120B**, 133 (1983).

[19] M. Dine and W. Fischler, The not-so-harmless axion, Phys. Lett. **120B**, 137 (1983).

[20] M. Kamionkowski, J. Pradler, and D. G. Walker, Dark Energy from the String Axiverse, Phys. Rev. Lett. **113**, 251302 (2014).

[21] S. Afach *et al.*, Search for topological defect dark matter using the global network of optical magnetometers for exotic physics searches (GNOME), Nat. Phys. **17**, 1396 (2021).

[22] S. Borsanyi *et al.*, Calculation of the axion mass based on high-temperature lattice quantum chromodynamics, Nature (London) **539**, 69 (2016).

[23] G. Ballesteros, J. Redondo, A. Ringwald, and C. Tamarit, Unifying Inflation with the Axion, Dark Matter, Baryogenesis, and the Seesaw Mechanism, Phys. Rev. Lett. **118**, 071802 (2017).

[24] V. B. Klaer and G. D. Moore, The dark-matter axion mass, J. Cosmol. Astropart. Phys. 11 (2017) 049.

[25] M. S. Turner, Windows on the axion, Phys. Rep. **197**, 67 (1990).

[26] A. Youdin, D. Krause, Jr., K. Jagannathan, L. Hunter, and S. Lamoreaux, Limits on Spin-Mass Couplings within the Axion Window, Phys. Rev. Lett. **77**, 2170 (1996).

[27] A. Arvanitaki and A. A. Geraci, Resonantly Detecting Axion-Mediated Forces with Nuclear Magnetic Resonance, Phys. Rev. Lett. **113**, 161801 (2014).

[28] Q. Yang, Probe dark matter axions using the hyperfine structure splitting of hydrogen atoms, arXiv:192.11472.

[29] T. Braine *et al.*, Extended Search for the Invisible Axion with the Axion Dark Matter Experiment, Phys. Rev. Lett. **124**, 101303 (2020).

[30] P. Gondolo and G. G. Raffelt, Solar neutrino limit on axions and keV-mass bosons, Phys. Rev. D **79**, 107301 (2009).

[31] G. G. Raffelt, Axion constraints from white dwarf cooling times, Phys. Lett. **166B**, 402 (1986).

[32] A. Ayala, I. Domínguez, M. Giannotti, A. Mirizzi, and O. Straniero, Revisiting the Bound on Axion-Photon Coupling from Globular Clusters, Phys. Rev. Lett. **113**, 191302 (2014).

[33] B. T. McAllister, G. Flower, E. N. Ivanov, M. Goryachev, J. Bourhill, and M. E. Tobar, The ORGAN experiment: An axion haloscope above 15 GHz, Phys. Dark Universe **18**, 67 (2017).

[34] A. P. Quiskamp, B. T. McAllister, P. Altin, E. N. Ivanov, M. Goryachev, and M. E. Tobar, Direct search for dark matter axions excluding ALP cogenesis in the 63-67 micro-eV range, with the ORGAN experiment, arXiv:2203.12152.

[35] P. Brun *et al.*, A new experimental approach to probe QCD axion dark matter in the mass range above 40 μeV, Eur. Phys. J. C **79**, 186 (2019).

[36] G. Rybka, A. Wagner, K. Patel, R. Percival, K. Ramos, and A. Brill, Search for dark matter axions with the orpheus experiment, Phys. Rev. D **91**, 011701(R) (2015).

[37] N. Aggarwal *et al.*, Characterization of magnetic field noise in the ariadne source mass rotor, Phys. Rev. Research **4**, 013090 (2022).

[38] X. Rong *et al.*, Searching for an exotic spin-dependent interaction with a single electron-spin quantum sensor, Nat. Commun. **9**, 739 (2018).

[39] W. Terrano, E. Adelberger, J. Lee, and B. Heckel, Short-Range, Spin-Dependent Interactions of Electrons: A Probe for Exotic Pseudo-Goldstone Bosons, Phys. Rev. Lett. **115**, 201801 (2015).

[40] B. R. Heckel, E. G. Adelberger, C. E. Cramer, T. S. Cook, S. Schlamminger, and U. Schmidt, Preferred-frame and C P-violation tests with polarized electrons, Phys. Rev. D **78**, 092006 (2008).

[41] P.-H. Chu, A. Dennis, C. B. Fu, H. Gao, R. Khatiwada, G. Laskaris, K. Li, E. Smith, W. M. Snow, H. Yan, and W. Zheng, Laboratory search for spin-dependent short-range force from axionlike particles using optically polarized ^{3}He gas, Phys. Rev. D **87**, 011105(R) (2013).

[42] M. Bulatowicz, R. Griffith, M. Larsen, J. Mirijanian, C. B. Fu, E. Smith, W. M. Snow, H. Yan, and T. G. Walker, Laboratory Search for a Long-Range T-Odd, P-Odd Interaction from Axionlike Particles Using Dual-Species Nuclear Magnetic Resonance with Polarized ^{129}Xe and ^{131}Xe Gas, Phys. Rev. Lett. **111**, 102001 (2013).

[43] Y. Stadnik, V. Dzuba, and V. Flambaum, Improved Limits on Axionlike-Particle-Mediated P, T-Violating Interactions between Electrons and Nucleons from Electric Dipole Moments of Atoms and Molecules, Phys. Rev. Lett. **120**, 013202 (2018).

[44] H. Yan, G. A. Sun, J. Gong, B. B. Pang, Y. Wang, Y. W. Yang, J. Zhang, and Y. Zhang, Probing the short range spin dependent interactions by polarized ^{3}He atom beams, Eur. Phys. J. C **74**, 3088 (2014).
[45] D. Wineland, J. Bollinger, D. Heinzen, W. Itano, and M. Raizen, Search for Anomalous Spin-Dependent Forces Using Stored-Ion Spectroscopy, Phys. Rev. Lett. **67**, 1735 (1991).
[46] A. G. Glenday, C. E. Cramer, D. F. Phillips, and R. L. Walsworth, Limits on Anomalous Spin-Spin Couplings between Neutrons, Phys. Rev. Lett. **101**, 261801 (2008).
[47] P. Fadeev, F. Ficek, M. G. Kozlov, D. Budker, and V. V. Flambaum, Pseudovector and pseudoscalar spin-dependent interactions in atoms, Phys. Rev. A **105**, 022812 (2022).
[48] G. Vasilakis, J. Brown, T. Kornack, and M. Romalis, Limits on New Long Range Nuclear Spin-Dependent Forces Set with a K-^{3}He Comagnetometer, Phys. Rev. Lett. **103**, 261801 (2009).
[49] M. Ledbetter, M. V. Romalis, and D. J. Kimball, Constraints on Short-Range Spin-Dependent Interactions from Scalar Spin-Spin Coupling in Deuterated Molecular Hydrogen, Phys. Rev. Lett. **110**, 040402 (2013).
[50] S. Kotler, R. Ozeri, and D. F. J. Kimball, Constraints on Exotic Dipole-Dipole Couplings between Electrons at the Micrometer Scale, Phys. Rev. Lett. **115**, 081801 (2015).
[51] F. Ficek, Derek F. Jackson Kimball, M. G. Kozlov, N. Leefer, S. Pustelny, and D. Budker, Constraints on exotic spin-dependent interactions between electrons from helium fine-structure spectroscopy, Phys. Rev. A **95**, 032505 (2017).
[52] B. Heckel, W. Terrano, and E. Adelberger, Limits on Exotic Long-Range Spin-Spin Interactions of Electrons, Phys. Rev. Lett. **111**, 151802 (2013).
[53] A. Almasi, J. Lee, H. Winarto, M. Smiciklas, and M. V. Romalis, New Limits on Anomalous Spin-Spin Interactions, Phys. Rev. Lett. **125**, 201802 (2020).
[54] W. Ji, Y. Chen, C. Fu, M. Ding, J. Fang, Z. Xiao, K. Wei, and H. Yan, New Experimental Limits on Exotic Spin-Spin-Velocity-Dependent Interactions by Using $SmCo_5$ Spin Sources, Phys. Rev. Lett. **121**, 261803 (2018).
[55] H. Su, Y. Wang, M. Jiang, W. Ji, P. Fadeev, D. Hu, X. Peng, and D. Budker, Search for exotic spin-dependent interactions with a spin-based amplifier, Sci. Adv. **7**, eabi9535 (2021).
[56] L. Hunter, J. Gordon, S. Peck, D. Ang, and J.-F. Lin, Using the earth as a polarized electron source to search for long-range spin-spin interactions, Science **339**, 928 (2013).
[57] J. Ding *et al.*, Constraints on the Velocity and Spin Dependent Exotic Interaction at the Micrometer Range, Phys. Rev. Lett. **124**, 161801 (2020).
[58] G. Raffelt, Limits on a C P-violating scalar axion-nucleon interaction, Phys. Rev. D **86**, 015001 (2012).
[59] B. A. Dobrescu and I. Mocioiu, Spin-dependent macroscopic forces from new particle exchange, 11 J. High Energy Phys. (2006) 005.
[60] M. Jiang, W. Xu, Q. Li, D. Suter, and X. Peng, Interference in atomic magnetometry, Adv. Quantum Technol. **3**, 2000078 (2020).
[61] M. Jiang, R. P. Frutos, T. Wu, J. W. Blanchard, X. Peng, and D. Budker, Magnetic Gradiometer for the Detection of Zero-to Ultralow-Field Nuclear Magnetic Resonance, Phys. Rev. Applied **11**, 024005 (2019).
[62] H. An, M. Pospelov, J. Pradler, and A. Ritz, Direct detection constraints on dark photon dark matter, Phys. Lett. B **747**, 331 (2015).
[63] See Supplemental Material at http://link.aps.org/supplemental/10.1103/PhysRevLett.129.051801 containing details of spin sensor, spin source, numerical simulation of the exotic pseudomagnetic field, and data analysis, which includes Ref. [64].
[64] M. V. Romalis, E. Miron, and G. D. Cates, Pressure broadening of rb D_1 and D_2 lines by ^{3}He, ^{4}He, N_2, and Xe: Line cores and near wings, Phys. Rev. A **56**, 4569 (1997).
[65] M. Jiang, H. Su, Z. Wu, X. Peng, and D. Budker, Floquet maser, Sci. Adv. **7**, eabe0719 (2021).
[66] T. G. Walker and W. Happer, Spin-exchange optical pumping of noble-gas nuclei, Rev. Mod. Phys. **69**, 629 (1997).
[67] W.-T. Ni, S.-s. Pan, H.-C. Yeh, L.-S. Hou, and J. Wan, Search for an Axionlike Spin Coupling Using a Paramagnetic Salt with a dc SQUID, Phys. Rev. Lett. **82**, 2439 (1999).
[68] D. J. Kimball, Nuclear spin content and constraints on exotic spin-dependent couplings, New J. Phys. **17**, 073008 (2015).
[69] M. Jiang, Y. Qin, X. Wang, Y. Wang, H. Su, X. Peng, and D. Budker, Floquet Spin Amplification, Phys. Rev. Lett. **128**, 233201 (2022).
[70] J. Lee, A. Almasi, and M. Romalis, Improved Limits on Spin-Mass Interactions, Phys. Rev. Lett. **120**, 161801 (2018).
[71] M. Padniuk, M. Kopciuch, R. Cipolletti, A. Wickenbrock, D. Budker, and S. Pustelny, Response of atomic spin-based sensors to magnetic and nonmagnetic perturbations, Sci. Rep. **12**, 324 (2022).
[72] H. Wu, S. Mirkhanov, W. Ng, and M. Oxborrow, Bench-Top Cooling of a Microwave Mode Using an Optically Pumped Spin Refrigerator, Phys. Rev. Lett. **127**, 053604 (2021).
[73] T. Theis, P. Ganssle, G. Kervern, S. Knappe, J. Kitching, M. P. Ledbetter, D. Budker, and A. Pines, Parahydrogen-enhanced zero-field nuclear magnetic resonance, Nat. Phys. **7**, 571 (2011).
[74] B. A. Dobrescu, Massless Gauge Bosons other than the Photon, Phys. Rev. Lett. **94**, 151802 (2005).
[75] S. Chaudhuri, P. W. Graham, K. Irwin, J. Mardon, S. Rajendran, and Y. Zhao, Radio for hidden-photon dark matter detection, Phys. Rev. D **92**, 075012 (2015).